ARTICLE OPEN

Check for updates

Environmental and developmental factors shape anti-AAV immunity in pigs

Godwin I. Iroanya[1], Ilangovan Raju[1,2], Chandra Boosani[1,2], Pradeep N. Subramanyam[1,2], Addison K. Byrne[1,2], Kevin D. Wells[1,2] and Jonathan A. Green[1,2]✉

Use of adeno-associated virus (AAV) vectors has revolutionized in vivo gene therapy, but the presence of pre-existing neutralizing antibodies remains a major barrier that can hinder clinical application. While large-animal models such as non-human primates have been used to study anti-AAV immunity, their high cost and limited accessibility present challenges for studying the impact of AAV immunity on AAV-based therapies. Here, we evaluate pigs as an immunologically relevant large-animal model for investigating humoral barriers to AAV-based gene therapy. Using ELISA-based profiling across 11 AAV serotypes, we detected immunoglobulin G (IgG) antibodies against AAV capsids in pigs as early as two weeks of age, with titers increasing with age and displaying serotype-specific dynamics. Animals maintained in standard housing displayed greater inter-individual variations and broader serotype-specific reactivities. Functional assays demonstrated that these antibodies neutralized AAV particles in a dose- and serotype-dependent manner, with IgG depletion restoring transduction in vitro. Sequence analysis indicated that capsid identity can partially predict cross-reactive binding, but only under controlled conditions. These findings establish pigs as a tunable model capable of recapitulating age- and environment-dependent features of anti-AAV immunity, providing a platform for studying humoral barriers and evaluating immune evasion strategies in AAV-based gene therapy.

Gene Therapy; https://doi.org/10.1038/s41434-026-00625-1

INTRODUCTION

Viral vectors based on adeno-associated viruses (AAVs) have emerged as a cornerstone in the development of in vivo gene therapies due to their favorable safety profile, broad tissue tropism, and capacity for long-term transgene expression [1–3]. AAV-based therapies have demonstrated clinical efficacy across a range of monogenic disorders, including hemophilia, spinal muscular atrophy, and retinal diseases [4–7]. However, the widespread implementation of AAV gene therapy is increasingly constrained by the presence of pre-existing neutralizing antibodies (NAbs) against AAV capsids, which can prevent vector transduction, reduce therapeutic efficacy, and lead to patient exclusion from clinical trials [8–10]. In many cases, even low-titer NAbs have been shown to substantially inhibit AAV-mediated gene delivery, underscoring the need for strategies that can either circumvent or mitigate humoral immunity [11, 12].

In humans and non-human primates (NHPs), anti-AAV immunity typically arises from natural exposure to wild-type AAV. Seroprevalence increases with age and is shaped by geographic region, co-infections, sanitation, and early-life environmental exposures [10, 12–14]. While rodent models have been invaluable in vector development, they exhibit fundamental immunological and anatomical differences from humans. These differences include impaired generation of primary and recall humoral responses with IgG class switching, limited T cell responses, incomplete development of key innate immune populations (monocytes, macrophages, dendritic cells, and NK cells), deficient complement activity, and poorly developed lymph node and germinal center architecture [15–17]. These differences limit the predictive value of rodents for rigorous preclinical testing of AAV immunogenicity and mitigation strategies. Large-animal models such as NHPs provide closer anatomical and immunological relevance but are costly, often limited in availability, and raise ethical concerns [18, 19].

In comparison, pigs represent a promising alternative large-animal model due to their immunological and physiological similarities to humans, genetic tractability, and suitability for longitudinal studies [20]. They have been increasingly used in biomedical research to study cardiovascular [21], metabolic [22], and infectious diseases [23], and are becoming popular as translational models for AAV-based therapies. Recent studies demonstrated that juvenile pigs can harbor pre-existing antibodies against a limited subset of AAV serotypes and that these antibodies can potentially impair vector transduction in vitro [24]. However, the extent and determinants of AAV immunity in pigs remain poorly characterized. It is unclear whether pigs exhibit the kind of serotype-specific and age-dependent immune patterns observed in humans, or whether immune profiles can be modulated by altering animal husbandry or management conditions. Without this knowledge, the full potential of the pig as a translational model for evaluating and mitigating humoral barriers to AAV gene therapy is unlikely to be achieved.

[1]Division of Animal Sciences, University of Missouri, Columbia, MO, USA. [2]National Swine Testing Center, University of Missouri, Columbia, MO, USA.
✉email: greenjo@missouri.edu

Received: 9 October 2025 Revised: 20 May 2026 Accepted: 20 May 2026
Published online: 29 May 2026

In this study, we expand upon previous observations by systematically characterizing the developmental and environmental factors that shape anti-AAV immunity in pigs. Using a panel of 11 AAV serotypes (AAV1, AAV2, AAV3, AAV4, AAV5, AAV6, AAV7, AAV8, AAV9, AAVrh10, also referred to as AAV10 in some commercial catalogs, and AAV11), we profiled serum antibody responses across multiple age groups and production environments, including both high-biosecurity and standard/conventional facilities. In addition to quantifying serotype-specific antibody titers, we assessed the functional neutralizing activity of pre-formed antibodies against AAV serotypes. Finally, we examined whether structural similarity among AAV capsids predicts patterns of cross-reactivity. Together, these efforts aim to establish pigs as a tunable and immunologically relevant large-animal model for preclinical testing of AAV gene therapies in the context of evaluating pre-existing humoral immunity that may interfere with gene therapy efforts.

MATERIALS AND METHODS

Sample collection

Whole blood samples were collected from independent Landrace White pigs across five developmental timepoints, 0, 2, 4, 6, and 8 weeks of age ($n = 6$ per age group), housed under standard facility conditions. Sample sizes were determined based on cohort availability and feasibility within the institutional swine facility. No prior power calculation was performed. Following data collection, post hoc power analysis was conducted to assess whether group sizes were sufficient to detect observed differences in antibody titers between experimental conditions.

To evaluate the influence of management practices on anti-AAV immunity, additional blood samples were obtained from 6-week-old Landrace White pigs ($n = 8$ per group) raised in either a standard pig housing facility or a high biosecurity facility. Animals in the high-biosecurity system were maintained under a strict "shower-in/shower-out" protocol, with personnel required to shower upon entry, and with no external clothing, footwear, or personal items permitted inside the facility. All incoming equipment and husbandry materials were cleaned extensively with disinfectants, and feed was sterilized by irradiation prior to entry. These measures were designed to minimize environmental and personnel-mediated microbial exposure, thereby providing a controlled setting to assess how reduced antigenic exposure influences the development of anti-AAV antibody responses.

Blood was collected via jugular venipuncture into serum tubes and centrifuged at 2000 rpm for 10 min at room temperature to isolate serum. Serum samples were aliquoted into labeled cryovials and stored at −20 °C until further analysis.

Enzyme-linked immunosorbent assay (ELISA)

An indirect ELISA was performed to quantify serum IgG antibodies specific to AAV capsids. High-binding polystyrene 96-well plates (Corning, Corning, NY, USA) were coated overnight at 4 °C with recombinant AAV capsids (vendors, serotypes and catalog numbers are listed in supplementary Table S1) at 1×10^9 viral particles per well (i.e., 100 µL of 1×10^{10} particles/mL in PBS, pH 7.4). Plates were washed three times using a 1X wash buffer composed of 154 mM NaCl, 24.7 µM thimerosal, and 0.05% (v/v) Tween-20, delivered via a BioTek 50 | TS microplate washer (Agilent Technologies Inc., Santa Clara, CA, USA).

Wells were blocked with 5% bovine serum albumin (BSA) in PBS containing 0.05% Tween-20 (PBST) and incubated for 60 min at 25 °C with gentle rocking, consistent with standard antibody binding assays. Serum samples were diluted in blocking buffer and added to the wells, followed by a 90-min incubation under the same conditions. Because anti-AAV IgG levels differed between cohorts, higher dilutions (1:5000) were required for samples with stronger binding signals, such as those from animals housed under standard conditions. In contrast, lower dilutions (1:500) were used for cohorts with weaker signals (animals from high-biosecurity housing). The dilution factors used for the evaluations were established empirically to ensure that sample reactivities were within the linear range of the assay.

Two rabbit polyclonal antibodies served as positive controls: a broadly reactive anti-AAV VP1/VP2/VP3 antibody (Progen, Heidelberg, Germany, Cat. #61084), which recognizes multiple AAV serotypes, and an anti-AAV5 VP3 (Invitrogen, Carlsbad, CA, USA. Cat. #PA5-22817), which is predominantly reactive to AAV5 and shows weak cross-reactivity with other serotypes. Both antibodies were diluted 1:500. The anti-VP1/VP2/VP3 antibody was used to confirm capsid coating and assay functionality across all serotypes tested, whereas the anti-AAV5 VP3 antibody was included to assess serotype-restricted binding specificity. Fetal porcine serum and 5% BSA were included as negative controls.

After washing, wells were incubated with horseradish peroxidase (HRP)-conjugated secondary antibodies for 60 min. Goat anti-pig IgG H&L (HRP) (Abcam, Waltham, MA, USA. Cat. #ab6915) was used at 1:5000 to detect porcine IgG, and Peroxidase AffiniPure Goat Anti-Rabbit IgG (H + L) (Jackson ImmunoResearch, West Grove, Pennsylvania, USA. Cat. #111-035-144) was used at the same dilution for rabbit control antibodies.

Colorimetric detection was performed using TMB substrate (Surmodics, Eden Prairie, MN, USA, Lot #TMBW240013), and reactions were stopped after 5 min using stop solution (Invitrogen, Lot #312960-000). Absorbance was measured at 450 nm using a BioTek Epoch 2 microplate reader. Raw optical density (OD) values were corrected by subtracting background absorbance from negative control wells.

Validation and dilution optimization

To ensure assay accuracy and reproducibility, we validated the ELISA platform using a monoclonal antibody standard, specificity testing, and serial dilution analysis. A standard curve generated with a purified monoclonal antibody against AAV5 VP3 showed robust linearity ($R^2 = 0.9996$), confirming the assay's quantitative capability. Specificity testing across 11 serotypes demonstrated strong reactivity only to AAV5 with minimal cross-reactivity.

For serum dilution optimization, equal volumes of serum from eight 6-week-old pigs per facility (standard and high biosecurity) were pooled and titrated (1:10–1:50000) against AAV2 capsids. Pooling was performed solely for assay calibration to identify dilution ranges that maintained signal within the linear dynamic range of the ELISA, after which all experimental analyses were conducted on individual serum samples. Titrations were fit with a four-parameter log-logistic (4PL) model to estimate EC50. The standard-facility pool had an EC50 of 1:4 620 (95% CI in Supplementary Fig. S1), and subsequent assays were performed at 1:5000 (1.08× EC50). The high-biosecurity pool had an EC50 of 1:273 (95% CI in Supplementary Fig. S2), and assays were performed at 1:500 (1.83× EC50). These dilutions maintained OD values within the linear range and avoided saturation.

IgG depletion and validation

To determine the contribution of IgG to AAV neutralization, porcine IgG was selectively removed using Protein A/G magnetic beads (Thermo Fisher Scientific, Waltham, MA, USA. Cat. #88803). Serum from 6-week-old pigs with high anti-AAV2 reactivity was incubated with pre-washed beads at a 1:1 (v/v) ratio for 1 h at room temperature with gentle rotation. Beads were separated magnetically, and the IgG-depleted supernatant was collected.

IgG depletion was confirmed by ELISA, using plates coated with AAV2 capsids (1×10^9 vg/well). Pre- and post-depletion serum samples (1:500 dilution) were probed with HRP-conjugated goat anti-pig IgG H&L antibodies (Abcam, Cat. #ab6915). A marked reduction in OD confirmed successful depletion.

For functional validation, NIH/3T3 cells were transduced with rAAV2 pre-incubated with IgG-depleted serum, untreated serum, or fetal porcine serum.

Cell culture

NIH/3T3 cells (ATCC, Manassas, VA, USA. CRL-1658) were cultured in Dulbecco's Modified Eagle Medium (DMEM; Gibco, Grand Island, NY, USA) supplemented with 10% fetal bovine serum (FBS; Gibco) and 0.5% GlutaMAX (Gibco). Cells were maintained at 37 °C in a humidified atmosphere with 5% CO_2 and passaged at 70–80% confluency using Accutase (Innovative Cell Technologies, San Diego, CA, USA).

AAV neutralization assay

To evaluate the functional impact of pre-existing antibodies on AAV transduction, a cell-based neutralization assay was performed using NIH/3T3 cells and recombinant AAV vectors encoding green fluorescent protein (GFP). Cells were seeded in 24-well plates at a density of 0.05×10^6 cells/well and cultured overnight in DMEM supplemented with 10% FBS and 0.5% GlutaMAX.

Recombinant AAV2, AAV6, AAV8, AAV9, and AAV11 vectors (Table S1) were applied at a fixed multiplicity of infection (MOI) of 1×10^3 vector

genomes (vg) per cell. This constant MOI was used to standardize viral genome input across serotypes. Viral titers were confirmed by genome copy quantification prior to use. No adjustments were made to equalize transduction output (e.g., GFP expression) between serotypes, as differences in baseline transduction efficiency reflect intrinsic capsid properties and were accounted for through normalization during the assessment of antibody-mediated inhibition.

AAV5 was excluded from the neutralization analyses because robust GFP expression could not be achieved under these standardized conditions. As normalization of transduction required a measurable baseline signal, the absence of reliable GFP expression precluded accurate quantification of serum-mediated inhibition for this serotype.

Porcine serum samples were diluted in FBS at ratios of 1:0 (porcine serum only), 1:9, 1:4, 2:3, and 0:1 (FBS only), and incubated with each tested rAAV for 1 h at 37 °C to allow antibody binding under physiologically relevant conditions. Virus–serum mixtures were then added to cells in triplicate wells.

After 48 h of incubation at 37 °C and 5% CO_2, cells were harvested using Accutase and analyzed for GFP expression by flow cytometry (Invitrogen Bigfoot Cell Sorter, Thermo Fisher Scientific). Transduction efficiency was quantified as the percentage of GFP-positive cells relative to total events.

For each serotype, a no-serum control condition (0:1) was used to establish baseline transduction. Transduction in the presence of serum was normalized to this control, which was set to 100%, and calculated as:

Relative Transduction (%) = (GFP-positive cells in serum-treated condition ÷ GFP-positive cells in no-serum control) × 100

This normalization strategy enabled comparison of the relative inhibitory effects of serum antibodies across serotypes independent of intrinsic differences in capsid-mediated transduction efficiency. Because porcine serum contains polyclonal antibodies with variable affinity and avidity for distinct capsid epitopes, normalization to a matched no-serum control ensured that observed reductions in transduction reflected antibody-mediated inhibition rather than differences in viral input or baseline infectivity.

Flow cytometry acquisition and analysis

At the specified time post-transduction, cells were washed with PBS, dissociated to a single-cell suspension using Accutase, and resuspended in flow buffer (PBS supplemented with 1% FBS). Samples were acquired on an Invitrogen Bigfoot Cell Sorter (Thermo Fisher Scientific) using a 488-nm laser, and GFP fluorescence was collected on the FITC channel. Non-transduced cells were used to define background autofluorescence and establish the GFP-positive threshold; single-stained controls were used for compensation when applicable. At least 10000 events were collected per sample.

Flow cytometry data were analyzed using the instrument's analysis software. Gating was performed sequentially to exclude debris based on forward and side scatter, followed by visualization of single-cell events using FSC height versus FSC area. GFP-positive and GFP-negative populations were defined based on fluorescence intensity using SSC versus GFP dot plots and confirmed by one-dimensional GFP histograms. Because the analysis was focused on quantifying transduction efficiency rather than cell sorting, singlet discrimination was not strictly enforced to maximize the number of events analyzed.

Sequence retrieval and multiple sequence alignment

AAV capsid protein sequences for serotypes AAV1 through AAV9 and AAVrh10 were retrieved from the UniProt Knowledgebase (UniProtKB) using the following accession numbers: AAV1 (Q9WBP8), AAV2 (Q87087), AAV3 (QDH44565.1), AAV4 (Q9J4G2), AAV5 (Q9JJZ2), AAV6 (Q9J4G0), AAV7 (Q8BHD3), AAV8 (Q8BHD2), AAV9 (Q8BHD1), and AAVrh10 (G3UUT3). Full-length amino acid sequences were aligned using Clustal Omega (https://www.ebi.ac.uk/Tools/msa/clustalo/), with manual segmentation into the VP1 unique region (VP1u), VP1/VP2 common region, and VP3 region. AAV11 was excluded from the sequence identity analysis due to the lack of a reliable, full-length capsid sequence suitable for comparative alignment.

Pairwise sequence identity analysis and visualization

Alignments were processed in R (version 4.3.1) using the Biostrings package to compute pairwise sequence identity matrices. Heatmaps were generated using the pheatmap package and hierarchically clustered to assess relationships among AAV serotypes. Sequence identity was evaluated for full-length capsids and subdomains to assess correlation with serological cross-reactivity.

In parallel, ELISA antibody reactivity profiles were compiled for each serotype across all serum samples, and pairwise Pearson correlation coefficients between serotypes were calculated based on these reactivity profiles. Pairwise sequence identity matrices were then compared with the corresponding serological correlation matrices to assess the relationship between capsid similarity and antibody cross-reactivity.

Statistical analysis

All statistical analyses were conducted in R (version 4.3.1). Linear mixed-effects models (LMMs) were used to evaluate the effects of Age, Serotype, and Facility on ELISA OD values and neutralization outcomes using the lme4 package. Random effects included Pig_ID (individual variation within and across litters) and/or Sow_ID (maternal influence), depending on design.

To evaluate differences in antibody levels across developmental stages and serotypes, LMMs were fitted with age and serotype as fixed effects and pig identity nested within sow identity as random effects. Because the nested sow-level effect was estimated near zero and produced singular fits, the final model used a pig-level random intercept. The model was specified as: $\text{Corrected\_OD}_{ijkl} = \mu + \alpha_i + \beta_j + (\alpha\beta)_{ij} + \mu_k + \epsilon_{ijkl}$, where μ is the overall mean, α_i is the fixed effect of age, β_j is the fixed effect of serotype, $(\alpha\beta)_{ij}$ is their interaction, $\mu_k \sim N(0,\sigma^2)$ is the pig-level random intercept, and ϵ_{ijkl} is the residual error. Post hoc pairwise comparisons were performed using estimated marginal means with Tukey adjustment for multiple comparisons.

Model assumptions were evaluated through residual diagnostics. Homogeneity of variance was assessed by visual inspection of residual-versus-fitted plots and by Levene's tests across serotype groups, which did not detect statistically significant variance differences. Simulation-based diagnostics using the DHARMa package further supported appropriate dispersion. Sensitivity analyses using log-transformed ELISA values yielded consistent results, indicating that conclusions were robust to potential mild heteroscedasticity.

Variance component analysis was done using restricted maximum likelihood (REML). Simulation-based power analyses were conducted using the simr package (nsim = 100) for two scenarios: (1) detecting Age × Serotype interactions using longitudinal ELISA data ($n = 30$ pigs across five ages); and (2) detecting inter-facility differences in serotype reactivity at 6 weeks of age ($n = 16$).

Pearson correlation coefficients (r) were used to assess the relationship between ELISA OD values and AAV transduction efficiency. Correlation matrices and visualizations were generated using ggplot2 and pheatmap.

Unless otherwise noted, results are presented as mean ± standard error of the mean (SEM), with $\alpha = 0.05$ considered statistically significant.

RESULTS

Detection of pre-existing anti-AAV antibodies in early and late postnatal stages in pigs

To assess the ontogeny of anti-AAV immunity in pigs, serum samples from standard facility-housed animals were collected at five developmental stages (fetal blood at 0 weeks, and postnatal ages 2, 4, 6, and 8 weeks; $n = 6$ per stage). IgG binding to 11 AAV serotypes was quantified using an indirect enzyme-linked immunosorbent assay (ELISA) at a fixed serum dilution of 1:500, which was necessary to enable detection of the lower reactivity in younger animals. Detectable IgG reactivity was observed as early as 2 weeks of age, with background-corrected optical density (OD) values increasing progressively with age for most serotypes (Fig. 1). AAV5 exhibited a transient response, with peak reactivity at 2 weeks followed by a decline.

ANOVA of the mixed-effects model identified age as the dominant predictor of antibody levels ($F(4,25) = 558.2$, $p = 4.8 \times 10^{-24}$), followed by serotype effects ($F(10, 250) = 56.5$, $p = 1.7 \times 10^{-58}$) and a highly significant age × serotype interaction ($F(40, 250) = 21.8$, $p = 5.8 \times 10^{-61}$) (Supplementary Table S2). Variance component analysis of the mixed-effects model indicated that fixed effects of age and serotype together accounted for 87.6% of the explained variance in ELISA reactivity, whereas the random effect associated with maternal origin (Sow_ID) contributed only 0.6%. Tukey-adjusted pairwise comparisons identified significant differences in optical densities between age groups within most serotypes ($p < 0.05$).

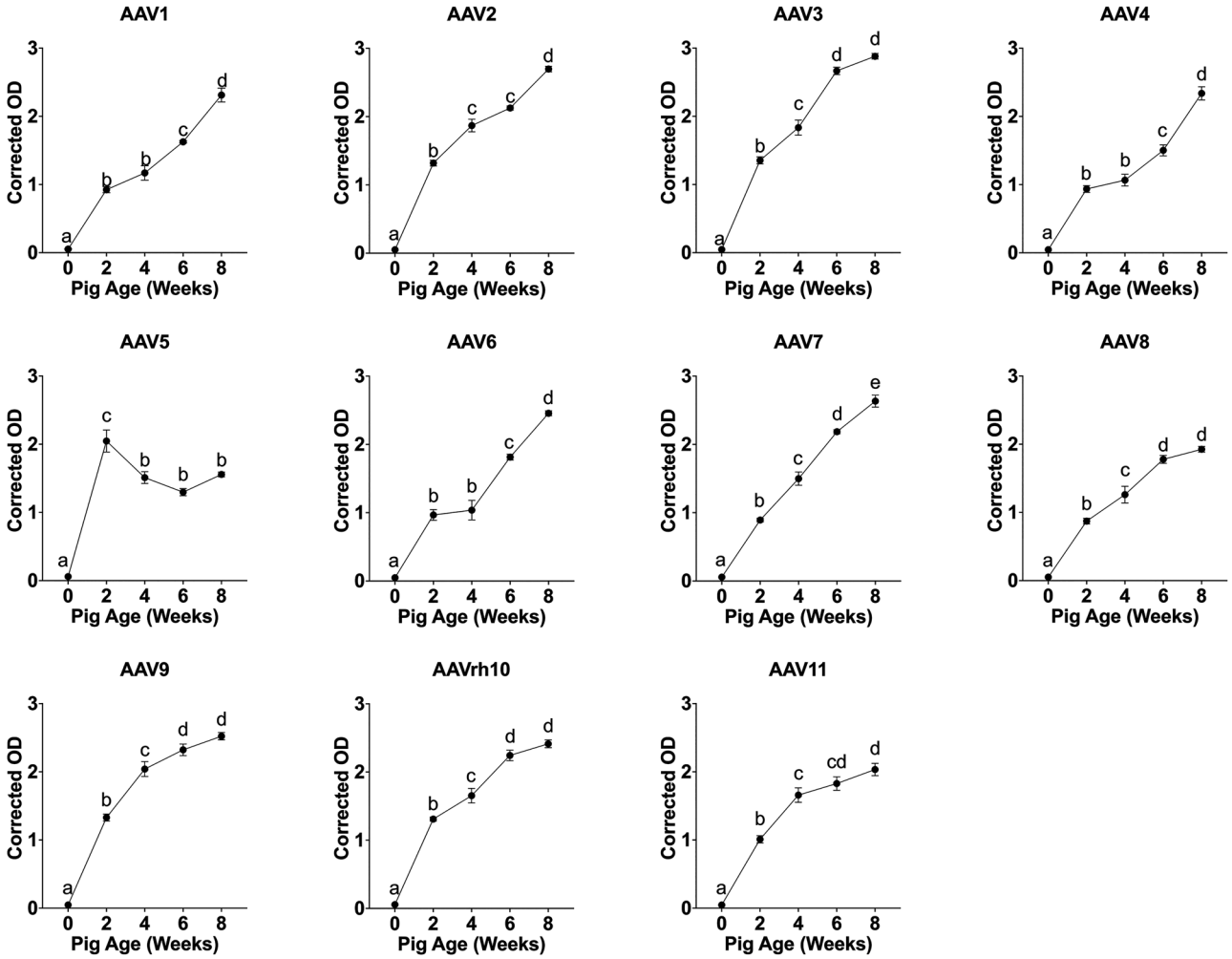

Fig. 1 Age-related antibody reactivity to AAV serotypes in pigs. Mean corrected optical density (OD ± standard error) values for 11 AAV serotypes (AAV1–AAV11) measured by indirect ELISA in serum from pigs housed in the standard facility. Samples were collected at five developmental stages (0, 2, 4, 6, and 8 weeks; $n = 6$ pigs per age group) and assayed at a fixed serum dilution of 1:500. Each panel represents a single AAV serotype. Different letters above denote statistically significant differences among ages within each serotype (mixed-effects model with Tukey's post hoc test, $p < 0.05$).

Antibody reactivity across AAV serotypes and facility conditions

To assess differences in anti-AAV antibody reactivity across serotypes and environmental conditions, we selected a cross-sectional cohort of 6-week-old pigs ($n = 8$) for analysis. This age represents a common window for vector delivery in preclinical studies and exhibited strong antibody signals in the prior longitudinal dataset (Fig. 1). To ensure measurements remained within the linear dynamic range of the ELISA and to avoid saturation, facility-specific serum dilutions determined by prior dilution optimization were used: 1:5000 for pigs raised in standard housing and 1:500 for pigs raised in high-biosecurity conditions.

Corrected OD values from each cohort were analyzed across AAV serotypes. Statistically significant variation was observed in antibody binding across the 11 tested serotypes in both facility groups (Fig. 2A, B). In the standard facility cohort, serotypes exhibited differing median corrected OD values with non-overlapping Tukey groupings (Fig. 2A). Similarly, in the high-biosecurity cohort, antibody responses varied significantly among serotypes with distinct statistical groupings (Fig. 2B).

To confirm that the experimental design was adequately powered to detect serotype-specific effects, a post hoc simulation-based power analysis was performed using a linear mixed-effects model (Corrected_OD ~ Serotype + (1 | Pig_ID)). The model achieved 100% power (95% CI: 96.4–100%) with 16 pigs (8 per facility) and 11 serotypes at $\alpha = 0.05$ (simr, nsim = 100).

To evaluate the effect of rearing conditions on antibody magnitude, corrected OD values at 1:5000 dilution were compared between the standard and high-biosecurity groups. Estimated marginal means were calculated using a linear model with a Serotype × Facility interaction term (Fig. 2C). A significant main effect of facility was observed ($p < 0.01$), indicating that the antibody levels were elevated in standard-facility pigs compared with high-biosecurity pigs.

Environmental exposure shapes serotype-specific antibody profiles and immune diversity

To examine the effect of housing conditions on serotype-specific antibody ranking and inter-individual variability, we compared antibody binding profiles using serum samples of pigs raised in high-biosecurity versus standard-biosecurity facility conditions at 6 weeks of age.

In the high-biosecurity cohort, within-pig ranking of corrected OD values across the 11 AAV serotypes was largely conserved

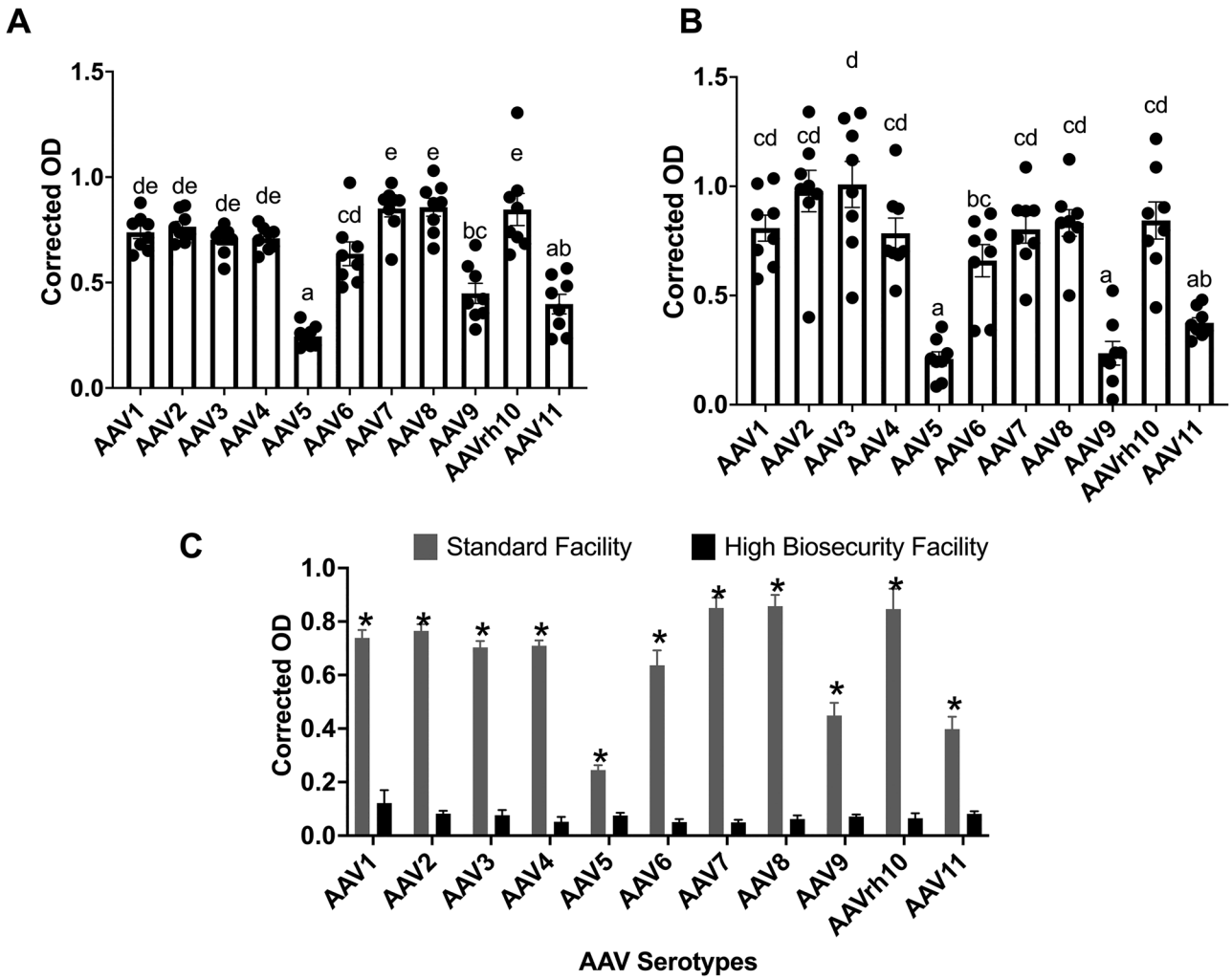

Fig. 2 Antibody reactivity to AAV serotypes and facility effects in 6-week-old pigs. A Standard Facility cohort ($n = 8$ pigs). Boxplots of blank-corrected OD from indirect ELISA measured at a 1:5000 serum dilution, comparing IgG reactivity across 11 AAV serotypes (AAV1–AAV11). Points are individual animals; boxes show median and IQR; whiskers are 1.5×IQR; black diamonds mark means. Letters indicate Tukey-adjusted groupings from the statistical model ($\alpha = 0.05$). **B** High Biosecurity Facility cohort ($n = 8$ pigs). Boxplots as in (**A**), comparing IgG reactivity across AAV serotypes, measured at a 1:500 serum dilution. **C** Facility comparison using common serum dilution (1:5000). Shown are estimated marginal means (EMMs; model-adjusted values, not raw means) of background-corrected OD for each serotype by facility (gray, Standard Facility; black, High Biosecurity Facility) derived from a model including Serotype, Facility, and interaction. Bars show EMMs with standard-error error bars; letters denote Tukey-adjusted comparisons between facilities within each serotype ($\alpha = 0.05$). Serotypes are ordered AAV1 → AAV11 in all panels.

across individuals. Most animals exhibited peak reactivity to AAV2 and AAV3, with low reactivity to AAV5 (Fig. 3B). Although absolute OD magnitude varied, the relative ordering of serotype reactivity was largely conserved across individuals.

In contrast, pigs raised in the standard facility displayed greater heterogeneity in rank-order patterns (Fig. 3A). The serotype exhibiting the highest relative reactivity varied among individual animals; however, AAV6, AAV7, AAV8, and AAVrh10 consistently occupied the top four rank positions among pigs raised under standard conditions. AAV5 and AAV11 consistently ranked lowest in relative reactivity in pigs raised under standard housing.

This variation was visualized by plotting within-animal rank orders of corrected OD values rather than absolute signal magnitude. Under high-biosecurity conditions, pigs exhibited greater concordance in rank order profiles across serotypes, whereas standard-housed pigs exhibited more animal-to-animal divergence in these rank patterns, which was consistent with these animals having more heterogeneous environmental exposure histories.

Antibody binding profiles reflect composite features across the AAV capsid

To investigate the relationship between AAV capsid sequence similarity and antibody cross-reactivity, we generated heatmaps comparing pairwise capsid amino acid sequence identity with pairwise correlations of ELISA antibody reactivity across serotypes. As shown in Fig. 4A, pairwise amino acid identity across full-length AAV capsid proteins revealed high conservation among several serotypes, with AAV1 and AAV6 (99%) forming one closely related group and AAV8 and AAVrh10 (93%) forming another. In contrast, AAV5 and AAV4 were more distantly related to other serotypes.

Serum antibody reactivity profiles were assessed by ELISA in pigs raised under high-biosecurity (Fig. 4B) and standard facility conditions (Fig. 4C). Pearson correlation matrices revealed that under high-biosecurity conditions, where pigs are likely to be more immunologically naive, patterns of cross-reactivity broadly reflected capsid sequence similarity. For instance, AAV3 and

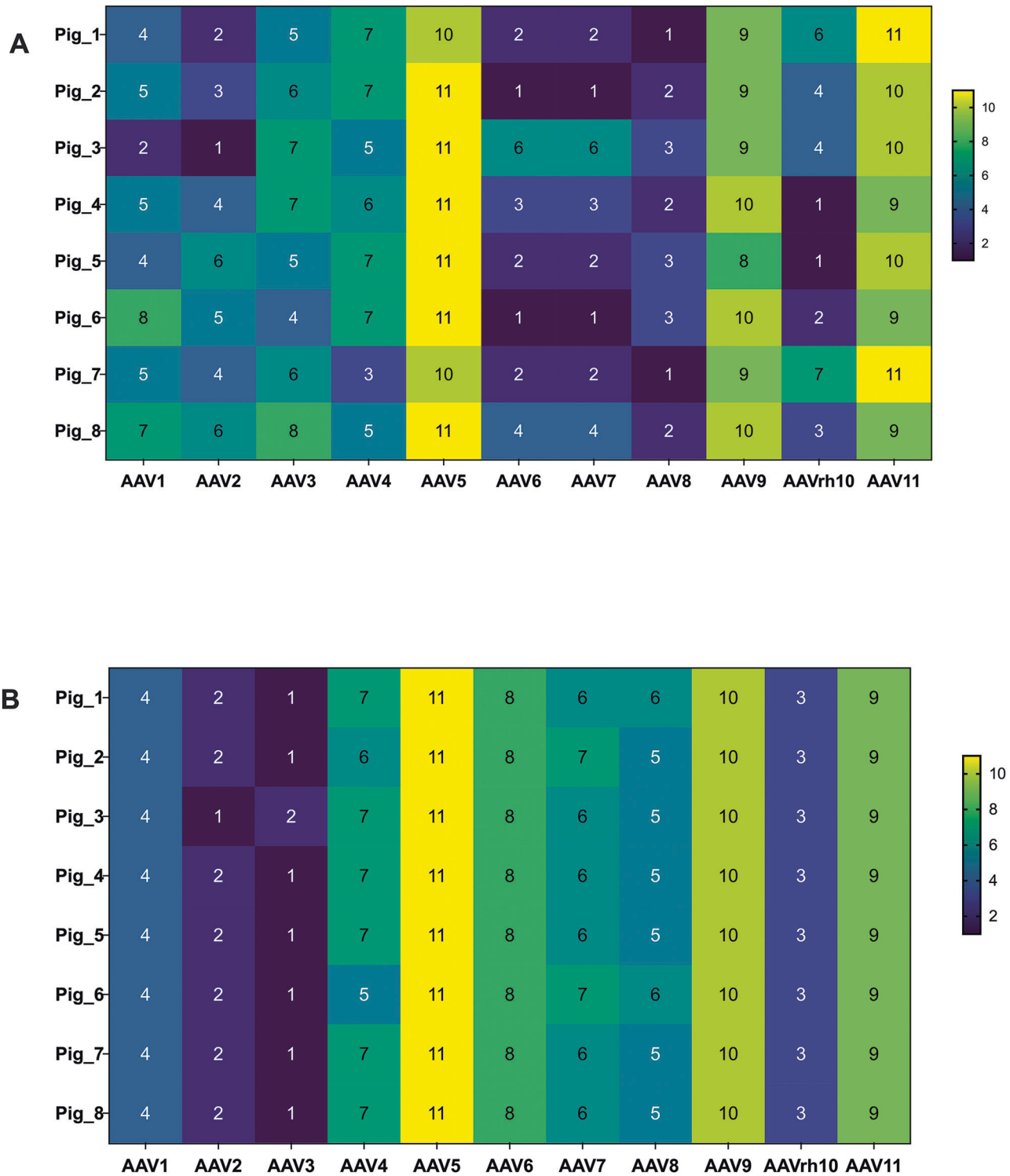

Fig. 3 Within-pig ranking of ELISA reactivity across AAV serotypes by facility and dilution. A Standard Facility cohort, serum dilution 1:5 000. Sera from 6-week-old pigs ($n = 8$ per panel) were assayed against 11 serotypes (AAV1–AAV11). For each pig (rows), corrected OD values were ranked across serotypes (1 = highest binding, 11 = lowest). Numbers inside tiles show the rank; the color scale runs from dark purple (rank 1) to yellow (rank 11). **B** High Biosecurity Facility cohort, serum dilution 1:500.

AAVrh10, which share >86% capsid identity, showed high serological correlation ($r = 0.73$), while AAV4 and AAV5, the most divergent pair, showed weak or negative correlation. However, under standard housing conditions, this relationship was less consistent, and this could be due to several other factors, such as immune imprinting, polyclonal diversification, or environmental exposure to cross-reactive antigens.

To quantify this relationship, we fit linear regression models using serotype-wise antibody correlation coefficients as the response variable and sequence identity across different capsid

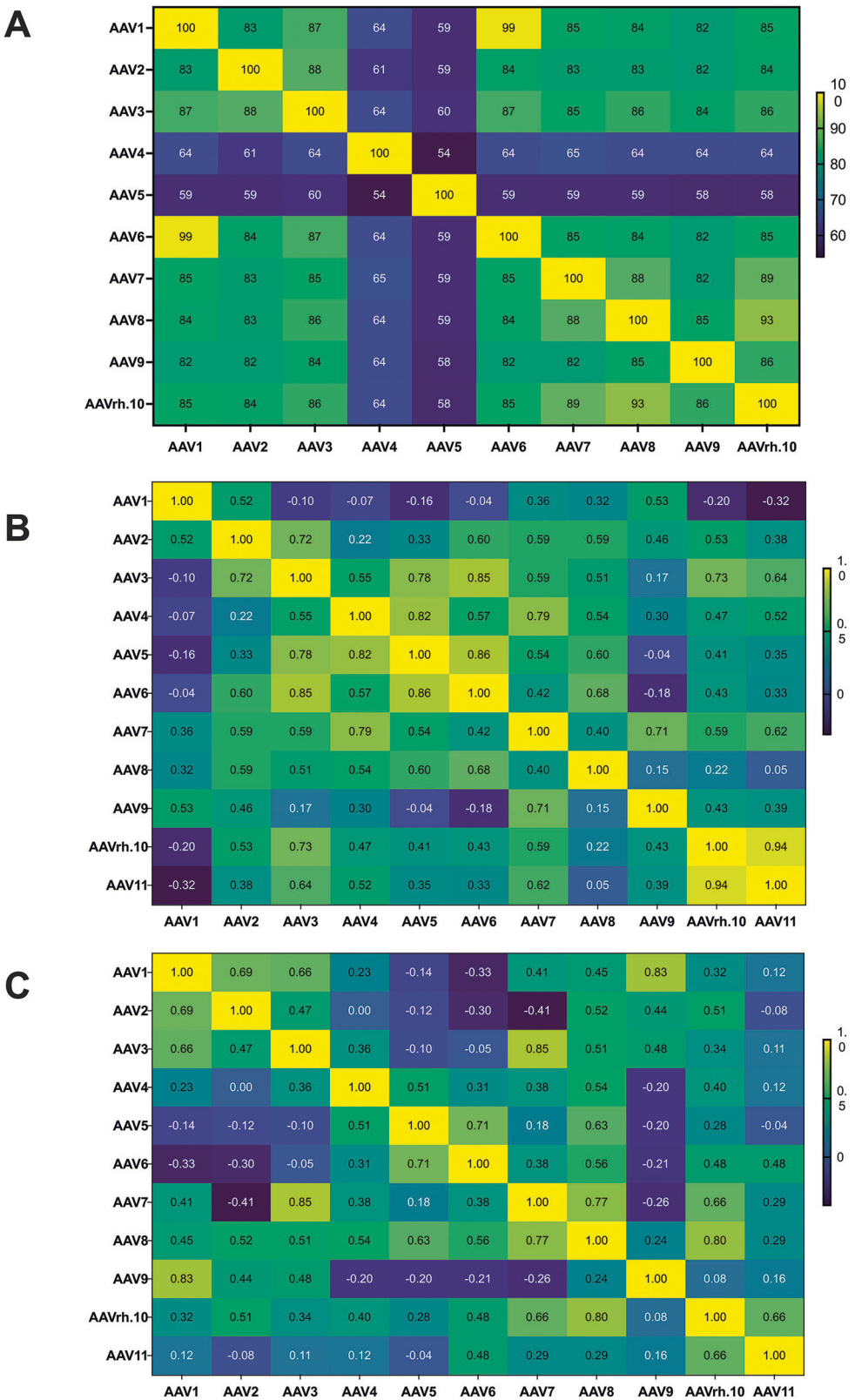

Fig. 4 Structural and functional relationships among AAV serotypes. A Heatmap of pairwise capsid sequence identity (AAV1–AAV10). Amino-acid identities were computed with Clustal Omega across full-length VP1/VP2/VP3 and displayed with hierarchical clustering. **B** Heatmap of pairwise Pearson correlations among anti-AAV IgG ELISA signals across serotypes for 6-week-old pigs from the High Biosecurity Facility cohort. **C** Same correlation matrix for the Standard Facility cohort. For (**B, C**), tiles show Pearson's r; serotype order and color scale are consistent across panels.

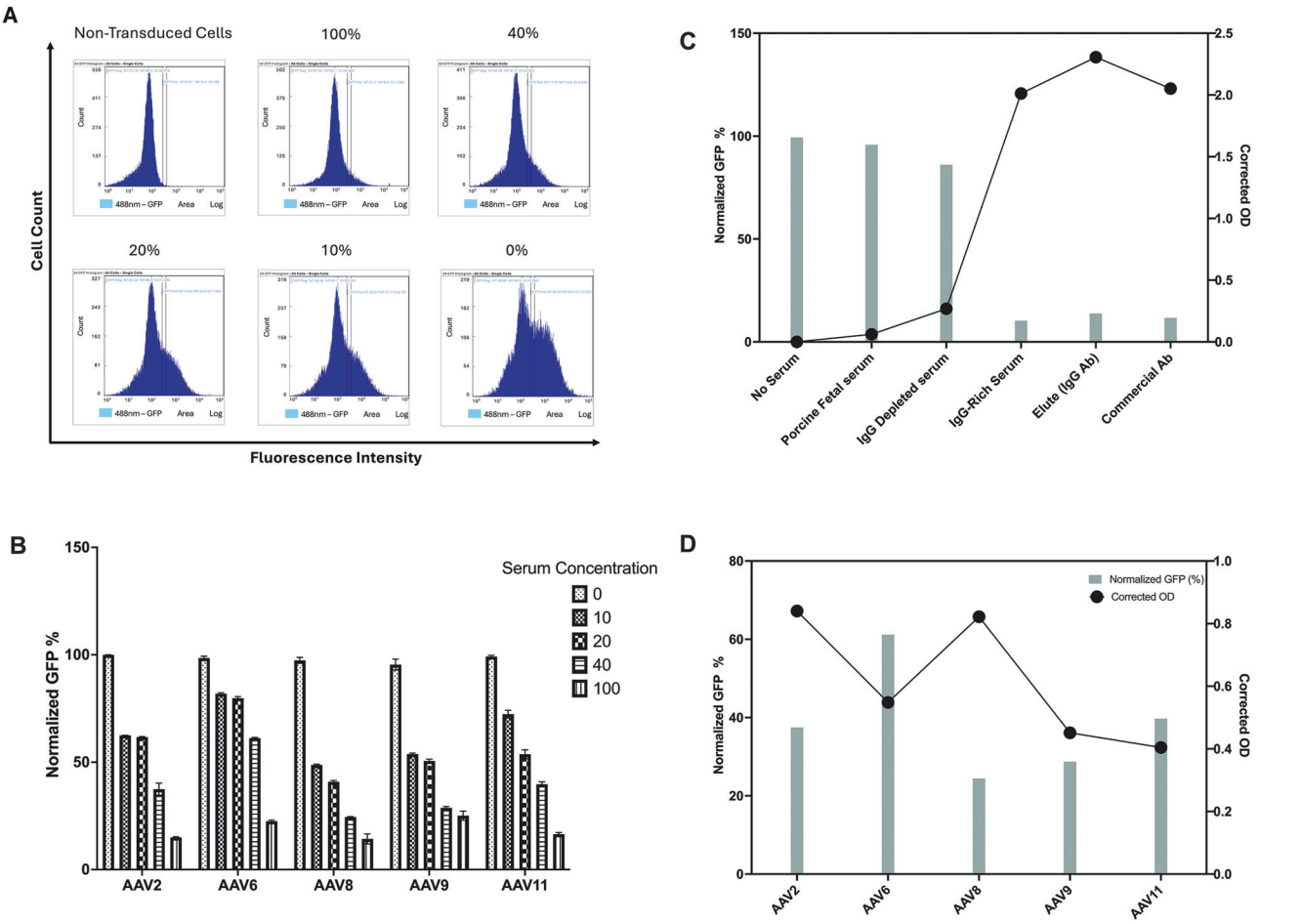

Fig. 5 Functional assays of serum-mediated neutralization and IgG depletion (standard facility). A Representative flow-cytometry histogram of GFP fluorescence in NIH/3T3 cells transduced with rAAV2-GFP, shown for a non-transduced control and for cells incubated with porcine serum from the standard facility at the indicated concentrations (10%, 20%, 40%, 100%). **B** Bar plots showing neutralization of AAV2, AAV6, AAV8, AAV9, and AAV11 by porcine serum from a standard facility. Normalized GFP (%) plotted against serum concentration (0–100%). Bars indicate mean ± SEM across replicates; fill patterns distinguish serotypes. **C** Effect of antibody fractionation on rAAV2 transduction and ELISA binding using serum from pigs housed in a standard facility. Bars show normalized GFP (%) for each sample group (Commercial Ab, Elute [IgG Ab], IgG-Rich Serum, IgG-Depleted Serum, No Serum, Porcine Fetal Serum). The dashed black line with dots indicates corrected OD (right y-axis). **D** Normalized GFP (%) at 40% serum for the same serotypes, with corrected OD values overlaid as black dots/line on the secondary (right) axis.

regions (VP1u, VP1/VP2 common region, VP3, and full capsid) as predictors:

$$\text{Serological Correlation}_{ij} = \beta_0 + \beta_1 \cdot \text{VP1}_{\text{uij}} + \beta_2 \cdot \text{VP1/VP2}_{ij} + \beta_3 \cdot \text{VP3}_{ij} + \beta_4 \cdot \text{FullCapsid}_{ij} + \epsilon_{ij}$$

In high-biosecurity pigs, the model explained 23% of the variance ($R^2 = 0.23$, $p = 0.028$), with full capsid identity showing the strongest positive association with serological similarity ($\beta = 0.015$). In contrast, no significant relationship was observed under standard conditions ($R^2 = 0.017$, $p = 0.95$), and all predictor coefficients were attenuated. Consistent with these results, sequence identity within individual capsid domains (VP1u, VP1/VP2 common region, or VP3) showed weaker associations with antibody reactivity than full capsid identity, indicating that no single capsid domain alone accounted for reactivity differences across serotypes.

In vitro neutralization activity of pre-existing antibodies and restoration of transduction by IgG depletion

To determine whether pre-existing anti-AAV antibodies in pigs are functionally neutralizing, serum samples from 6-week-old pigs were incubated with GFP-expressing recombinant AAV (rAAV) vectors and used to transduce NIH/3T3 cells. Transgene expression was quantified by flow cytometry and expressed as relative transduction normalized to the no-serum control for each serotype (set to 100%).

Incubation with undiluted porcine serum (100%) resulted in near-complete inhibition of transduction across all evaluated serotypes, as indicated by relative transduction values approaching zero (Fig. 5A). At lower serum concentrations (10% and 20%), partial inhibition was observed, with relative transduction increasing in a dose-dependent manner. In contrast, control conditions containing fetal bovine serum without porcine serum maintained maximal transduction (100%), confirming that the observed reduction in GFP expression was mediated by components present in porcine serum.

This dose-dependent inhibitory effect was consistently observed across AAV2, AAV6, AAV8, AAV9, and AAV11, although the magnitude of inhibition varied by serotype (Fig. 5B). AAV6 exhibited the highest relative transduction across serum concentrations, indicating relative resistance to antibody-mediated inhibition, whereas AAV8 and AAV9 showed greater susceptibility, with more pronounced reductions in relative transduction.

To identify the antibody class responsible for this effect, IgG was selectively depleted from porcine serum using Protein A/G magnetic beads. IgG depletion restored transduction to levels comparable to controls lacking porcine serum, with relative transduction values averaging approximately 85–95% (Fig. 5C). In contrast, IgG-enriched fractions and a commercial anti-AAV VP1/VP2/VP3 antibody (Progen, Cat. #61084) maintained strong inhibitory effects, confirming that IgG is the primary mediator of AAV neutralization in this system.

At an intermediate serum concentration (40%), serotype-specific differences in neutralization were further resolved (Fig. 5D). AAV6 maintained the highest relative transduction, while AAV8 and AAV9 exhibited substantial inhibition.

To assess whether antibody binding magnitude predicted functional neutralization, ELISA-derived corrected OD values were compared with relative transduction across serotypes. An inverse relationship was observed for several serotypes, including AAV2, AAV6, and AAV8, indicating that higher antibody binding was generally associated with greater inhibition of transduction. However, this relationship was not uniform across all serotypes. For example, AAV6, AAV9, and AAV11 exhibited comparable ELISA reactivity but differed in relative transduction, indicating that antibody binding magnitude alone does not fully predict neutralization efficacy. These findings suggest that additional factors, including antibody affinity, avidity, and epitope specificity, contribute to the functional outcome of AAV–antibody interactions.

DISCUSSION

This study demonstrated that pigs naturally develop anti-AAV antibodies in an age- and environment-dependent manner, thus offering a tunable large-animal model for studying pre-existing immunity in the context of AAV gene therapy. We systematically profiled humoral responses across eleven AAV serotypes and examined their specificity, variability, and functional correlations. Our findings showed that pigs recapitulate key features of anti-AAV immunity seen in humans and non-human primates (NHPs), while providing the experimental accessibility necessary for translational research.

Serotype-specific antibody responses reflect developmental and maternal influences

Our longitudinal analysis demonstrates that under the rearing conditions tested here, pigs naturally develop anti-AAV antibodies early in life, with IgG responses detectable as early as two weeks of age and progressively increasing thereafter. This age-associated rise was evident across multiple AAV serotypes, including AAV1, AAV2, and AAV8, which are the serotypes that have also shown high seroprevalence in both humans and non-human primates [25, 26]. The observed dynamics closely parallel those reported in human and NHP studies, where age is a key determinant of seroconversion magnitude [13, 14, 25–27].

Importantly, 6-week-old pigs should not be considered immunologically immature in the same manner as juvenile non-human primates. Pigs undergo rapid postnatal immune development and, by this age, possess a functionally active adaptive immune system capable of endogenous IgG production [28–30]. Thus, the presence of anti-AAV IgG across multiple serotypes at six weeks of age, including in animals raised under high-biosecurity conditions, likely reflects a composite immune landscape, shaped by overlapping contributions from maternally derived antibodies, early endogenous immune responses, and cross-reactive recognition of shared AAV capsid epitopes [26, 31]. While high-biosecurity housing limits environmental exposures, it is not a sterile environment and does not render the animals immunologically naïve.

Interestingly, AAV5 exhibited a nonlinear reactivity pattern, with antibody titers being the greatest at two weeks of age before declining. This trajectory strongly suggests a maternal origin for the anti-AAV5 antibodies. In mammals, it is well established that IgG is transferred from mother to offspring, particularly through colostrum in the neonatal period [32, 33]. In pigs, the epitheliochorial placenta prevents transplacental transfer of immunoglobulins. Consequently, neonates are agammaglobulinemic at birth [34]. In these animals, passive immunity is acquired exclusively through colostrum ingestion within the first 24–36 h after birth, during which intestinal permeability allows systemic uptake of maternal IgG [34–36]. In the context of AAV, human infants have been shown to possess high titers of AAV9 antibodies in early life that decline rapidly within the first few months after birth [37]. Our findings suggest that the AAV5 reactivity observed in two-week-old piglets is likely maternally derived, consistent with passive transfer of immunity. This pattern mirrors what is seen in human infants, where maternally acquired IgG dominates the early immune landscape before waning over time [14, 37]. Moreover, given that AAV5 is among the least immunogenic serotypes in humans [11], early peaks in antibody titer likely reflect declines in circulating maternal antibodies rather than active seroconversion. This raises an important and underexplored question in gene therapy: to what extent does maternally derived immunity impact the efficacy and timing of vector administration in neonates and young animals? Understanding this influence could guide the development of optimized gene therapy strategies for early-life interventions.

In contrast with the changes in titer to AAV5, the sustained increase in antibodies against serotypes such as AAV2 and AAV8 likely represents de novo immune responses initiated as piglets begin to encounter these serotypes in their environment. These divergent serotype-specific trajectories provide critical insight into the ontogeny of anti-AAV immunity and highlight the pig as a compelling model for studying pediatric immune development in gene therapy contexts.

Housing conditions modulate antibody breadth and inter-individual variability

Our findings reveal that the housing environment is a major determinant of both the magnitude and diversity of anti-AAV antibodies detected in pigs. Animals raised under high-biosecurity conditions, which are marked by restricted microbial exposure and tightly controlled husbandry, exhibited lower overall reactivity and greater consistency in the rank-order pattern of serotype recognition across individuals, despite variability in absolute signal magnitude. In this cohort, pigs showed consistent antibody binding to AAV2 and AAV3, with minimal recognition of AAV5.

In contrast, pigs raised in standard farm environments displayed higher antibody titers, broader serotype recognition, and substantially greater inter-individual heterogeneity in rank order and absolute signal magnitude. Within this group, some animals mounted dominant responses to AAV2, AAV8, and AAVrh10, while others exhibited diverse and idiosyncratic reactivity patterns across multiple serotypes. This divergence highlights the role of environmental antigens in shaping the porcine humoral immune landscape.

These observations are consistent with epidemiological trends in humans, where factors such as geography and early-life microbial exposure significantly influence anti-AAV seroprevalence and antibody breadth [13, 38]. For instance, anti-AAV2 seroprevalence is significantly higher in sub-Saharan Africa compared to the United States [10], and children with early school attendance, a proxy for increased environmental contact, have been shown to harbor higher antibody titers [13]. Similarly, non-human primates exposed to conventional microbial environments develop broader and more robust anti-AAV immunity compared to their counterparts maintained in specific-pathogen-free conditions [38]. The findings presented here capture both ends of this immunological spectrum: high-biosecurity pigs serve as a reproducible baseline

for controlled immunogenicity studies, while standard-housed pigs reflect the immune complexity and heterogeneity seen in outbred human populations.

Importantly, serotype-specific trends in pigs mirrored those reported in humans and NHPs, reinforcing the translational relevance of this model. AAV5 consistently showed low immunogenicity across both housing environments, echoing the minimal seroprevalence that has been observed in human and primate studies [38].

Capsid sequence similarity provides correlative and predictive antibody profiles under controlled conditions

To investigate the structural basis of serotype-specific antibody recognition, we examined the relationship between AAV capsid sequence identity and antibody binding profiles. In pigs raised under high-biosecurity conditions, where immune exposures are minimized, and immune histories are presumed naive, we observed a modest correlation between antibody binding and overall capsid sequence similarity, particularly within the full-length capsid and the VP1/VP2 regions. This suggests that in immunologically naive animals, conserved surface-exposed epitopes may partially guide humoral recognition, and is in agreement with prior findings in humans and non-human primates [38, 39].

However, no single capsid domain fully accounted for the observed binding patterns. Rather, antibody recognition appeared to arise from a composite of structural and sequence features distributed across the capsid, including conformational epitopes formed by variable loops and higher-order capsid assembly, as has been demonstrated for AAV and icosahedral viruses [39–41]. Importantly, this modest sequence-binding correlation largely broke down in pigs housed under standard conditions. In this context, broader antigenic exposure, polyclonal diversification, immune imprinting, or cross-reactivity with non-AAV antigens, if present, may have obscured the relationship between sequence and immune recognition patterns, underscoring the complex interplay between environment and immunity.

Interestingly, the VP3 region, despite forming the structural core of the AAV capsid and encompassing several variable loops implicated in antigenicity [41, 42], appeared to be a poor predictor of antibody binding. This may be due to its high degree of conservation across serotypes, limiting its contribution to serotype-specific recognition. Similarly, the VP1 unique region (VP1u), known for its role in endosomal escape and transient externalization during infection [41, 43], did not show high predictive value for antibody reactivity in isolation. These observations are consistent with emerging structural studies indicating that immunodominant epitopes are conformational rather than linear, often clustered at the 3-fold and 5-fold axes of symmetry, and shaped by capsid arrangement, protein glycosylation, and host-specific B cell repertoires [39, 44, 45].

Notably, the lack of correlation between VP1u similarity and antibody binding in our ELISA assays may also suggest that steric blockade of cell receptor engagement is not the dominant neutralization mechanism in pigs. Because many anti-AAV antibodies recognize conformational epitopes presented on intact capsids, enhancing assay resolution through approaches that probe binding strength, such as avidity measurements or increasingly stringent chaotropic urea wash steps applied to intact capsids, may improve our ability to dissect differences in anti-capsid interactions without assuming linear epitope recognition.

Together, these findings highlight that antibody recognition is governed by structural conformation and immunological context rather than capsid sequence alone. As such, predictive models based solely on sequence identity may be insufficient to fully capture the complexity of humoral immunity to AAV vectors, particularly under conditions of diverse antigenic exposure. It is also possible that the modest correlations observed, especially under high-biosecurity conditions, could become more robust with a larger sample size (N), which would increase statistical power and reduce the influence of outlier animals. Such refinement may be particularly relevant in uncovering subtle trends that are otherwise masked by individual variability in immune responses.

Functional neutralization by IgG can be reversed by antibody depletion

Beyond capsid binding, our findings support previous reports that pre-existing anti-AAV antibodies in pigs are functionally neutralizing. In addition to the broad neutralization capabilities reported, our study examines serotype specificity within the neutralization component of immune mediation. Sera from 6-week-old animals inhibited the transduction of NIH/3T3 cells by recombinant AAV vectors in a serotype- and dose-dependent manner. The degree of inhibition varied across serotypes, with AAV8 and AAV9 being most susceptible, and AAV6 demonstrating partial resilience. These serotype-specific differences in neutralization susceptibility suggest that certain capsid features, such as surface charge, epitope accessibility, or conformational flexibility, may modulate vulnerability to antibody-mediated blockade, consistent with patterns observed in human and NHP studies [10, 46, 47].

Importantly, the neutralization profiles observed here highlight a distinction between capsid-binding activity and functional inhibition. While ELISA assays revealed high levels of anti-AAV IgG binding at substantial serum dilutions, effective neutralization required higher serum concentrations, indicating that a significant fraction of capsid-binding antibodies may be non-neutralizing or weakly neutralizing. This phenomenon has been widely reported in clinical and preclinical gene therapy studies and underscores the importance of functional assays for assessing the biological relevance of serological responses [9, 48, 49].

We further confirmed that the inhibitory activity in 6-week-old pig sera is IgG-mediated. Depletion of serum IgG using Protein A/G beads restored AAV2 transduction to near-baseline levels, while the IgG-enriched fraction retained inhibitory capacity (Fig. 5C). These results echo previous reports in both clinical and preclinical settings, where IgG is the dominant isotype responsible for neutralizing AAV vectors through extracellular blockade and Fc-dependent pathways [50–53].

The experimental flexibility of the pig model also enables mechanistic dissection and therapeutic intervention at a scale and level of environmental and procedural control that is not feasible in human studies and is substantially more limited in non-human primate models. IgG depletion, as demonstrated here, provides a foundation for testing clinically relevant mitigation strategies, such as plasmapheresis, decoy capsids, and transient immunosuppression [50, 51]. While such approaches are often limited to in vitro testing or small-animal models, pigs offer a scalable, immunologically relevant, and ethically acceptable system for in vivo validation. This is particularly valuable for studies requiring invasive sampling, longitudinal antibody tracking, or direct tissue-level assessment of transgene expression and vector biodistribution.

Moreover, the adaptability of the pig model across housing environments allows investigators to tailor experimental contexts to their research goals. Under high-biosecurity conditions, pigs exhibited uniform antibody profiles dominated by AAV2 and AAV3, paralleling constrained neutralizing patterns seen in pediatric humans and NHPs raised under specific pathogen-free (SPF) conditions [14, 26]. This uniformity makes them ideal for benchmarking neutralization thresholds and evaluating dose-responsiveness of mitigation tools under tightly controlled conditions. Conversely, pigs raised under standard farm conditions displayed variable serotype hierarchies and neutralizing capacities dominated by AAV8 or AAVrh10 responses. This reflects the immune imprinting from environmental antigen exposure, akin to the heterogeneity seen in diverse human populations [12, 15].

Future directions and limitations

The present study provides environmental and developmental insights into the origins, diversity, and functional consequences of pre-existing anti-AAV immunity in pigs. By systematically dissecting the influence of age, housing environment, and capsid sequence similarity, we identify pigs as a tunable and translationally relevant model for studying humoral barriers to AAV gene therapy. Our data demonstrates that porcine IgG antibodies develop early, vary by serotype, differ by biosecurity level, and are functionally neutralizing in a dose-dependent manner. These findings not only mirror key immunological trends observed in humans and non-human primates but also position the pig as a useful preclinical platform for immune profiling and therapeutic intervention.

However, some limitations in this study should be noted. While we characterized IgG-mediated neutralization from serotype-specific perspectives, we did not evaluate other antibody effector mechanisms such as complement activation, antibody-dependent cellular cytotoxicity (ADCC), or TRIM21-mediated intracellular restriction [54–56], as these are beyond the scope of the present work. Likewise, high-resolution epitope mapping and profiling of the B cell repertoire underlying serotype-specific responses were not conducted but represent important directions for future studies. In addition, neutralization assays were conducted under standardized MOI and incubation conditions to enable within-serotype comparisons; under these conditions, robust transgene expression could not be achieved for AAV5, precluding its inclusion in functional neutralization analysis. Because intrinsic transduction efficiency varies across AAV serotypes, the use of a fixed MOI does not yield equivalent baseline transduction; therefore, comparisons across serotypes rely on normalized relative transduction rather than absolute GFP output and should be interpreted as relative measures of antibody-mediated inhibition rather than direct comparisons of absolute transduction efficiency. Furthermore, our functional assays were limited to in vitro systems; in vivo validation will be necessary to fully assess how pre-existing antibodies influence vector delivery, transgene expression, and therapeutic outcomes in target tissues.

Future work should include structural characterization of neutralizing epitopes using cryo-EM, investigation of non-IgG antibody classes and Fc-mediated effector functions, and in vivo testing of immune modulation strategies under both controlled and complex environmental conditions. Such studies will further refine our understanding of AAV immunogenicity and inform the rational development of next-generation vectors and mitigation strategies for gene therapy in diverse patient populations.

CONCLUSION

This study establishes pigs as a valuable and versatile large-animal model for characterizing pre-existing anti-AAV immunity and for evaluating immune-vector interactions and AAV-based therapeutics in a translationally relevant setting. We demonstrated that IgG antibodies against AAV capsids are present in pigs as early as two weeks of age, generally increase thereafter, and vary by serotype. The housing environment had a profound effect on antibody responses. Pigs raised under high-biosecurity conditions exhibited uniform, serotype-restricted immunity, while those raised in conventional facilities mounted broader responses with greater inter-individual variability. ELISA-based antibody binding was inversely correlated with vector transduction in vitro, and IgG depletion restored infectivity, confirming the neutralizing function of these pre-formed antibodies. Although capsid sequence similarity showed modest population-level association with antibody cross-reactivity under immunologically restricted conditions, this relationship was inconsistent at the level of individual serotype pairs and was disrupted in more complex immune environments, underscoring the influence of antigenic history on immune recognition.

Collectively, these findings position the pig as a powerful translational model for investigating humoral barriers to AAV gene therapy. Its capacity to simulate both controlled and heterogeneous immune states enables mechanistic dissection, high-throughput screening, and population-level immunological priming. Furthermore, pigs offer experimental flexibility and scalability for testing mitigation strategies, such as vector engineering, immune modulation, and decoy capsids, in ways that complement rodents and non-human primates by enabling larger cohorts, longitudinal sampling, and controlled exposure conditions. As the gene therapy field advances toward redosing, serotype switching, and personalized delivery strategies, the porcine model may provide a useful platform for optimizing efficacy and broadening clinical applicability.

DATA AVAILABILITY

The datasets generated and analyzed in the current study are available within the published article and its supplementary files. Additional data are available from the corresponding author upon reasonable request.

REFERENCES

1. Wang D, Tai PWL, Gao G. Adeno-associated virus vector as a platform for gene therapy delivery. Nat Rev Drug Discov. 2019;18:358–78. https://doi.org/10.1038/s41573-019-0012-9.
2. Kotterman MA, Schaffer DV. Engineering adeno-associated viruses for clinical gene therapy. Nat Rev Genet. 2014;15:445–51.
3. Li C, Samulski RJ. Engineering adeno-associated virus vectors for gene therapy. Nat Rev Genet. 2020;21:255–72. https://doi.org/10.1038/s41576-019-0205-4.
4. Ong T, Pennesi ME, Birch DG, Lam BL, Tsang SH. Adeno-associated viral gene therapy for inherited retinal disease. Pharmacol Res. 2019;36:34. https://doi.org/10.1007/s11095-018-2564-5.
5. Mendell JR, Al-Zaidy S, Shell R, Arnold WD, Rodino-Klapac LR, Prior TW, et al. Single-dose gene-replacement therapy for spinal muscular atrophy. N Engl J Med. 2017;377:1713–22.
6. Mount JD, Herzog RW, Tillson DM, Goodman SA, Robinson N, McCleland ML, et al. Sustained phenotypic correction of hemophilia B dogs with a factor IX null mutation by liver-directed gene therapy. Blood J Am Soc Hematol. 2002;99:2670–6.
7. Reiss UM, Davidoff AM, Tuddenham EGD, Chowdary P, McIntosh J, Muczynski V, et al. Sustained CLINICAL benefit of AAV gene therapy in severe hemophilia B. N Engl J Med. 2025;392:2226–34. https://doi.org/10.1056/NEJMoa2414783.
8. Greenberg B, Butler J, Felker GM, Ponikowski P, Voors AA, Pogoda JM, et al. Prevalence of AAV1 neutralizing antibodies and consequences for a clinical trial of gene transfer for advanced heart failure. Gene Ther. 2016;23:313–9. https://doi.org/10.1038/gt.2015.109.
9. Boutin S, Monteilhet V, Veron P, Leborgne C, Benveniste O, Montus MF, et al. Prevalence of serum IgG and neutralizing factors against adeno-associated virus (AAV) types 1, 2, 5, 6, 8, and 9 in the healthy population: implications for gene therapy using AAV vectors. Hum Gene Ther. 2010;21:704–12.
10. Calcedo R, Vandenberghe LH, Gao G, Lin J, Wilson JM. Worldwide epidemiology of neutralizing antibodies to adeno-associated viruses. J Infect Dis. 2009;199:381–90. https://doi.org/10.1086/595830.
11. Klamroth R, Hayes G, Andreeva T, Gregg K, Suzuki T, Mitha IH, et al. Global seroprevalence of pre-existing immunity against AAV5 and other AAV serotypes in people with hemophilia A. Hum Gene Ther. 2022;33:432. https://doi.org/10.1089/hum.2021.287.
12. Wang L, Calcedo R, Bell P, Lin J, Grant RL, Siegel DL, et al. Impact of pre-existing immunity on gene transfer to nonhuman primate liver with adeno-associated virus 8 vectors. Hum Gene Ther. 2011;22:1389–401.
13. Qin X, Li H, Zhao H, Xiang K, Liu S, Lou R, et al. Prevalence of neutralizing antibodies against AAV serotypes 2 and 9 in healthy participants from multiple centers across China and patients with DMD/BMD. Hum Gene Ther. 2024;35:969–77. https://doi.org/10.1089/hum.2024.079.
14. Perocheau DP, Cunningham SC, Lee J, Antinao Diaz J, Waddington SN, Gilmour K, et al. Age-related seroprevalence of antibodies against AAV-LK03 in a UK population cohort. Hum Gene Ther. 2019;30:79–87. https://doi.org/10.1089/hum.2018.098.
15. Brehm MA, Shultz LD, Luban J, Greiner DL. Overcoming current limitations in humanized mouse research. J Infect Dis. 2013;208:S125–30. https://doi.org/10.1093/infdis/jit319.

16. Bennett RS, Huzella LM, Jahrling PB, Bollinger L, Olinger GG, Hensley LE. Non-human primate models of Ebola virus disease. In: Mühlberger E, Hensley LL, Towner JS, editors. Marburg- and Ebolaviruses. Cham: Springer International Publishing; 2017. p. 171–93. Available from: http://link.springer.com/10.1007/82_2017_20. https://doi.org/10.1007/82_2017_20
17. Vuyyuru R, Patton J, Manser T. Human immune system mice: current potential and limitations for translational research on human antibody responses. Immunol Res. 2011;51:257–66. https://doi.org/10.1007/s12026-011-8243-9.
18. Ramos K, Downey A, Yost O. Nonhuman primate models in biomedical research: state of the science and future needs. The National Academies Press; 2023. Available from: https://nap.nationalacademies.org/catalog/26857/nonhuman-primate-models-in-biomedical-research-state-of-the-science
19. Carvalho C, Gaspar A, Knight A, Vicente L. Ethical and scientific pitfalls concerning laboratory research with non-human primates, and possible solutions. Animals. 2018;9:12. https://doi.org/10.3390/ani9010012.
20. Pabst R. The pig as a model for immunology research. Cell Tissue Res. 2020;380:287–304. https://doi.org/10.1007/s00441-020-03206-9.
21. Jia H, Chang Y, Song J. The pig as an optimal animal model for cardiovascular research. Lab Anim. 2024;53:136–47. https://doi.org/10.1038/s41684-024-01377-4.
22. Hou N, Du X, Wu S. Advances in pig models of human diseases. Anim Model Exp Med. 2022;5:141–52. https://doi.org/10.1002/ame2.12223.
23. Hayes BH, Andraud M, Salazar LG, Rose N, Vergne T. Mechanistic modeling of African swine fever: a systematic review. Prevent Vet Med. 2021;191:105358. https://doi.org/10.1016/j.prevetmed.2021.105358.
24. Dai Y, Kavita U, Lampen MH, Gielen S, Banks G, Levesque P, et al. Prevalence of pre-existing neutralizing antibodies against adeno-associated virus serotypes 1, 2, 5, 6, 8, and 9 in sera of different pig strains. Hum Gene Ther. 2022;33:451–9. https://doi.org/10.1089/hum.2021.213.
25. Leborgne C, Latournerie V, Boutin S, Desgue D, Quéré A, Pignot E, et al. Prevalence and long-term monitoring of humoral immunity against adeno-associated virus in Duchenne Muscular Dystrophy patients. Cell Immunol. 2019;342. 103780.
26. Wang X, Klann PJ, Wiedtke E, Sano Y, Fischer N, Schiller L, et al. Seroprevalence of binding and neutralizing antibodies against 18 adeno-associated virus types in patients with neuromuscular disorders. Front Immunol. 2024;15. 1450858. https://doi.org/10.3389/fimmu.2024.1450858.
27. Wei C, Li D, Zhang M, Zhao Y, Liu Y, Fan Y, et al. Prevalence of adeno-associated virus-9-neutralizing antibody in chinese patients with Duchenne muscular dystrophy. Hum Gene Ther. 2024;35:26–35. https://doi.org/10.1089/hum.2023.117.
28. Rothkötter HJ. Anatomical particularities of the porcine immune system—a physician's view. Dev Comp Immunol. 2009;33:267–72. https://doi.org/10.1016/j.dci.2008.06.016.
29. Šinkora M, Butler JE. The ontogeny of the porcine immune system. Dev Comp Immunol. 2009;33:273–83. https://doi.org/10.1016/j.dci.2008.07.011.
30. Butler JE, Sinkora M. The isolator piglet: a model for studying the development of adaptive immunity. Immunol Res. 2007;39:33–51. https://doi.org/10.1007/s12026-007-0062-7.
31. Calcedo R, Wilson JM. Humoral Immune Response to AAV. Front Immunol. 2013;4:341. https://doi.org/10.3389/fimmu.2013.00341
32. Albrecht M, Pagenkemper M, Wiessner C, Spohn M, Lütgehetmann M, Jacobsen H, et al. Infant immunity against viral infections is advanced by the placenta-dependent vertical transfer of maternal antibodies. Vaccine. 2022;40:1563–71. https://doi.org/10.1016/j.vaccine.2020.12.049.
33. Pou C, Nkulikiyimfura D, Henckel E, Olin A, Lakshmikanth T, Mikes J, et al. The repertoire of maternal anti-viral antibodies in human newborns. Nat Med. 2019;25:591–6. https://doi.org/10.1038/s41591-019-0392-8.
34. Rooke JA, Bland IM. The acquisition of passive immunity in the newborn piglet. Livest Prod Sci. 2002;78:13–23. https://doi.org/10.1016/S0301-6226(02)00182-3.
35. Salmon H, Berri M, Gerdts V, Meurens F. Humoral and cellular factors of maternal immunity in swine. Dev Comp Immunol. 2009;33:384–93. https://doi.org/10.1016/j.dci.2008.07.007. Mar 1.
36. Maciag SS, Bellaver FV, Bombassaro G, Haach V, Morés MAZ, Baron LF, et al. On the influence of the source of porcine colostrum in the development of early immune ontogeny in piglets. Sci Rep. 2022;12:15630. https://doi.org/10.1038/s41598-022-20082-1.
37. Day JW, Mendell JR, Burghes AHM, van Olden RW, Adhikary RR, Dilly KW. Adeno-associated virus serotype 9 antibody seroprevalence for patients in the United States with spinal muscular atrophy. Mol Ther Methods Clin Dev. 2023;31:101117. https://doi.org/10.1016/j.omtm.2023.101117.
38. Calcedo R, Wilson JM. AAV natural infection induces broad cross-neutralizing antibody responses to multiple AAV serotypes in chimpanzees. Hum Gene Ther Clin Dev. 2016;27:79–82. https://doi.org/10.1089/humc.2016.048.
39. Tseng YS, Agbandje-McKenna M. Mapping the AAV capsid host antibody response toward the development of second-generation gene delivery vectors. Front Immunol. 2014;5:9.
40. Gurda BL, DiMattia MA, Miller EB, Bennett A, McKenna R, Weichert WS, et al. Capsid antibodies to different adeno-associated virus serotypes bind common regions. J Virol. 2013;87:9111–24. https://doi.org/10.1128/jvi.00622-13.
41. Wobus CE, Hügle-Dörr B, Girod A, Petersen G, Hallek M, Kleinschmidt JA. Monoclonal antibodies against the adeno-associated virus type 2 (aav-2) capsid: epitope mapping and identification of capsid domains involved in AAV-2–cell interaction and neutralization of AAV-2 infection. J Virol. 2000;74:9281–93. https://doi.org/10.1128/jvi.74.19.9281-9293.2000.
42. Agbandje-McKenna M, Kleinschmidt J. AAV capsid structure and cell interactions. In: Snyder RO, Moullier P, editors. Adeno-associated virus: methods and protocols. Totowa: Humana Press; 2011. p. 47–92. Available from: https://doi.org/10.1007/978-1-61779-370-7_3
43. Powell SK, McCown TJ. Adeno-associated virus 9 (AAV9) viral proteins VP1, VP2, and membrane-associated accessory protein (MAAP) differentially influence in vivo transgene expression. J Virol. 2024;98:e01681-24. https://doi.org/10.1128/jvi.01681-24.
44. Mingozzi F, High KA. Immune responses to AAV vectors: overcoming barriers to successful gene therapy. Blood. 2013;122:23–36. https://doi.org/10.1182/blood-2013-01-306647.
45. Emmanuel SN, Smith JK, Hsi J, Tseng YS, Kaplan M, Mietzsch M, et al. Structurally mapping antigenic epitopes of adeno-associated virus 9: development of antibody escape variants. J Virol. 2022;96:e01251. https://doi.org/10.1128/JVI.01251-21.
46. Jeune VL, Joergensen JA, Hajjar RJ, Weber T. Pre-existing anti–adeno-associated virus antibodies as a challenge in AAV gene therapy. Hum Gene Ther Methods. 2013;24:59–67. https://doi.org/10.1089/hgtb.2012.243.
47. Gao GP, Alvira MR, Wang L, Calcedo R, Johnston J, Wilson JM. Novel adeno-associated viruses from rhesus monkeys as vectors for human gene therapy. Proc Natl Acad Sci USA. 2002;99:11854–9. https://doi.org/10.1073/pnas.182412299.
48. Rapti K, Louis-Jeune V, Kohlbrenner E, Ishikawa K, Ladage D, Zolotukhin S, et al. Neutralizing antibodies against AAV serotypes 1, 2, 6, and 9 in sera of commonly used animal models. Mol Ther. 2012;20:73–83. https://doi.org/10.1038/mt.2011.177
49. Hurlbut GD, Ziegler RJ, Nietupski JB, Foley JW, Woodworth LA, Meyers E, et al. Preexisting immunity and low expression in primates highlight translational challenges for liver-directed AAV8-mediated gene therapy. Mol Ther. 2010;18:1983–94. https://doi.org/10.1038/mt.2010.175.
50. Elmore ZC, Oh DK, Simon KE, Fanous MM, Asokan A. Rescuing AAV gene transfer from neutralizing antibodies with an IgG-degrading enzyme. JCI Insight. 5:e139881. https://doi.org/10.1172/jci.insight.139881
51. Smith TJ, Elmore ZC, Fusco RM, Hull JA, Rosales A, Martinez M, et al. Engineered IgM and IgG cleaving enzymes for mitigating antibody neutralization and complement activation in AAV gene transfer. Mol Ther. 2024;32:2080–93. https://doi.org/10.1016/j.ymthe.2024.05.004.
52. Lonze BE, Tatapudi VS, Weldon EP, Min ES, Ali NM, Deterville CL, et al. IdeS (Imlifidase): a novel agent that cleaves human IgG and permits successful kidney transplantation across high-strength donor-specific antibody. Ann Surg. 2018;268:488–96.
53. Iroanya GI, Subramanyam PN, Wells KD, Green JA. Pre-existing anti-adeno-associated virus immunity in gene therapy: mechanisms, challenges, and potential solutions. Hum Gene Ther. 2025;36:1463–80. https://doi.org/10.1177/10430342251378524.
54. Kropf E, Markusic DM, Majowicz A, Mingozzi F, Kuranda K. Complement system response to adeno-associated virus vector gene therapy. Hum Gene Ther. 2024;35:425–38. https://doi.org/10.1089/hum.2023.194.
55. Vogt MR, Dowd KA, Engle M, Tesh RB, Johnson S, Pierson TC, et al. Poorly neutralizing cross-reactive antibodies against the fusion loop of West Nile virus envelope protein protect in vivo via Fcgamma receptor and complement-dependent effector mechanisms. J Virol. 2011;85:11567–80. https://doi.org/10.1128/JVI.05859-11.
56. Smith CJ, Ross N, Kamal A, Kim KY, Kropf E, Deschatelets P, et al. Pre-existing humoral immunity and complement pathway contribute to immunogenicity of adeno-associated virus (AAV) vector in human blood. Front Immunol. 2022;13:999021. https://doi.org/10.3389/fimmu.2022.999021.

ACKNOWLEDGEMENTS

We thank the Immunology Core Facility, Laboratory for Infectious Disease Research (LIDR, University of Missouri, Columbia, MO), which assisted with the cytometry analysis.

AUTHOR CONTRIBUTIONS

GII participated in all aspects of sample collection, data generation, analysis, and initial drafting and subsequent editing of the manuscript. IR assisted with sample

processing and helped with ELISA assays and manuscript editing. CB participated in project planning, sample collection, analysis of results, and manuscript editing. PNS assisted with sample collection, analysis of results, and manuscript editing. AKB coordinated animal use, participated in project planning, data interpretation, and manuscript editing. KDW was involved in project conceptualization, data interpretation, and manuscript editing. JAG was involved in project conceptualization and overall supervision, data interpretation, and manuscript editing.

FUNDING

This work was supported in part by the National Institutes of Health (U42OD035738 and U42OD027090).

COMPETING INTERESTS

The authors declare no competing interests.

ETHICAL APPROVAL

All animal procedures were conducted in accordance with institutional and federal guidelines for the care and use of laboratory animals. The study was approved by the University of Missouri Institutional Animal Care and Use Committee. Animals were housed under controlled environmental conditions with ad libitum access to food and water. All blood collections were performed by trained personnel, and all efforts were made to minimize animal handling and discomfort.

ADDITIONAL INFORMATION

Supplementary information The online version contains supplementary material available at https://doi.org/10.1038/s41434-026-00625-1.

Correspondence and requests for materials should be addressed to Jonathan A. Green.